

Vacuum current-carrying tribological behavior of MoS_2-Ti films with different conductivities

Lu-Lu Pei(裴露露), Peng-Fei Ju(鞠鹏飞), Li Ji(吉利), Hong-Xuan Li(李红轩),Xiao-Hong Liu(刘晓红), Hui-Di Zhou(周惠娣), and Jian-Min Chen(陈建敏)

Citation: Chin. Phys. B, 2022, 31 (**6**): 066201. DOI: 10.1088/1674-1056/ac4f5a
Journal homepage: http://cpb.iphy.ac.cn; http://iopscience.iop.org/cpb

What follows is a list of articles you may be interested in

Reaction mechanism of metal and pyrite under high-pressure and high-temperature conditions and improvement of the properties

Yao Wang(王遥), Dan Xu(徐丹), Shan Gao(高姗), Qi Chen(陈启), Dayi Zhou(周大义), Xin Fan(范鑫), Xin-Jian Li(李欣健), Lijie Chang(常立杰),Yuewen Zhang(张跃文), Hongan Ma(马红安), and Xiao-Peng Jia(贾晓鹏)
Chin. Phys. B, 2022, 31 (**6**): 066206. DOI: 10.1088/1674-1056/ac4a72

Theoretical study of novel B-C-O compoundswith non-diamond isoelectronic

Chao Liu(刘超) and Pan Ying(应盼)
Chin. Phys. B, 2022, 31 (**2**): 026201. DOI: 10.1088/1674-1056/ac0cd2

Insights into the physical properties and anisotropic nature of ErPdBi with an appearance of low minimum thermal conductivity

S K Mitro, R Majumder, K M Hossain, Md Zahid Hasan, Md Emran Hossain, and M A Hadi
Chin. Phys. B, 2021, 30 (**1**): 016203. DOI: 10.1088/1674-1056/abaf9d

Utilizing of high-pressure high-temperature synthesis to enhance the thermoelectric properties of $Zn_{0.98}Al_{0.02}O$ with excellent electrical properties

Qi Chen(陈启), Xinjian Li(李欣健), Yao Wang(王遥), Lijie Chang(常立杰), Jian Wang(王健), Yuewen Zhang(张跃文), Hongan Ma(马红安), and Xiaopeng Jia(贾晓鹏)
Chin. Phys. B, 2021, 30 (**1**): 016202. DOI: 10.1088/1674-1056/abc4dd

Theoretical calculations of hardness and metallicity for multibond hexagonal 5d transition metal diborides with ReB_2 structure

Jun Yang(杨俊), Fa-Ming Gao(高发明), Yong-Shan Liu(刘永山)
Chin. Phys. B, 2017, 26 (**10**): 106202. DOI: 10.1088/1674-1056/26/10/106202

Vacuum current-carrying tribological behavior of MoS_2-Ti films with different conductivities

Lu-Lu Pei(裴露露)[1,2], Peng-Fei Ju(鞠鹏飞)[3], Li Ji(吉利)[1,†], Hong-Xuan Li(李红轩)[1,‡], Xiao-Hong Liu(刘晓红)[1], Hui-Di Zhou(周惠娣)[1], and Jian-Min Chen(陈建敏)[1]

[1] *Key Laboratory of Science and Technology on Wear and Protection of Materials, Lanzhou Institute of Chemical Physics, Chinese Academy of Sciences, Lanzhou* 730000, *China*

[2] *Center of Materials Science and Optoelectronics Engineering, University of Chinese Academy of Sciences, Beijing* 100049, *China*

[3] *Shanghai Aerospace Equipment Manufacture, Shanghai* 200245, *China*

(Received 21 December 2021; revised manuscript received 21 January 2022; accepted manuscript online 27 January 2022)

Current-carrying sliding is widely applied in aerospace equipment, but it is limited by the poor lubricity of the present materials and the unclear tribological mechanism. This study demonstrated the potential of MoS_2-based materials with excellent lubricity as space sliding electrical contact materials by doping Ti to improve its conductivity. The tribological behavior of MoS_2-Ti films under current-carrying sliding in vacuum was studied by establishing a simulation evaluating device. Moreover, the noncurrent-carrying sliding and static current-carrying experiments in vacuum were carried out for comparison to understand the tribological mechanism. In addition to mechanical wear, the current-induced arc erosion and thermal effect take important roles in accelerating the wear. Arc erosion is caused by the accumulation of electric charge, which is related to the conductivity of the film. While the current-thermal effect softens the film, causing strong adhesive wear, and good conductivity and the large contact area are beneficial for minimizing the thermal effect. So the moderate hardness and good conductivity of MoS_2-Ti film contribute to its excellent current-carrying tribological behavior in vacuum, showing a significant advantage compared with the traditional ones.

Keywords: MoS_2-Ti films, conductivity, current-carrying tribological behavior, vacuum

PACS: 62.20.Qp, 81.15.Cd **DOI:** 10.1088/1674-1056/ac4f5a

1. Introduction

Sliding electrical contact materials guarantee the transmission of signals and current of the space equipment, such as the slip ring for solar windsurfing. In selecting traditional sliding electrical contact materials, the focus is mainly on the electrical conductivity of the materials. Au is often used as a space sliding electrical contact material.[1–3] However, despite its excellent electrical conductivity, its service life fails to meet new requirements because of its insufficient lubricity[4] Thus, new sliding electrical contact materials should be developed. MoS_2 is an excellent space lubricating material, and it has been widely applied to the space environment.[5–7] Nonetheless, it remains limited because of its poor electrical conductivity. Fortunately, adding metals to MoS_2 films is considered as an effective method for improving not only their electrical properties but also their mechanical and tribological properties.[8–12] Ti is a good additive candidate because of its unique electrical and mechanical properties. Thus, MoS_2-Ti composite (MOST) films as sliding electrical contact materials were investigated in the current work.

The wear mechanism of sliding electrical contact materials is complex. It exists in the form of mechanical wear without load current and electrical wear with load current.[13–15] Moreover, many experiments have been conducted in an atmospheric environment, and some progress has been made with regard to the wear mechanism.[16–21] However, conducting current-carrying friction studies in vacuum, remains difficult thus far mainly because harsh and complex service environments, vacuum and current, are not easy to simulate. In the current study, a ball-on-disc reciprocating sliding vacuum tribometer equipped with a current control system was built to simulate a real space environment. The results should provide reliable guidance for the development of space sliding electrical contact materials.

Based on this, in the present study, Ti-doped MoS_2 films with different Ti contents were deposited using unbalanced magnetron sputtering equipment. Meanwhile, the behaviors of MOST films under current-carrying sliding, non-current-carrying sliding and static current-carrying conditions in vacuum were investigated. Finally, vacuum tribological mechanism of MOST films under current-carrying conditions was discussed.

2. Experiment details

2.1. Film preparation

MoS_2-Ti (MOST) composite films were deposited on substrates (mirror-polished Si (100) and stainless steel (Sus-304)) by using closed field unbalanced magnetron sputtering

†Corresponding author. E-mail: jili@licp.cas.cn

‡Corresponding author. E-mail: lihx@licp.cas.cn

© 2022 Chinese Physical Society and IOP Publishing Ltd

equipment (Teer plasma CF-800), with MoS_2 target and Ti target in argon (purity 99.99%) plasma. The substrates were sequentially cleaned with acetone and deionized water by using ultrasonic waves for 20 min and then dried. After the cleaning treatment, the substrates were transferred into a deposition chamber. The substrates were then cleaned by plasma etching with Ar ions for 20 min to remove the native oxides on the surface when the chamber pressure was below 3.0×10^{-3} Pa. A Ti interlayer with a thickness of 250 nm was deposited on the substrates by magnetron sputtering to enhance the adhesion strength of the substrate and films. Then, films with different Ti contents were prepared by tailoring the current of the Ti target. The sputtering current of the MoS_2 target was fixed at 1.2 A. The sputtering current settings of the Ti target were 0 A, 0.2 A, 0.4 A, 0.6 A and 0.8 A, and the corresponding samples were labelled as MOST-0%Ti, MOST-4%Ti, MOST-8%Ti, MOST-12%Ti, MOST-16%Ti, respectively. The MOST-0%Ti film was deposited for 3 h and other films were deposited for 4 h.

2.2. Evaluation of current-carrying tribological properties

Evaluating the current-carrying tribological properties of the films deposited on stainless steel by a CSM ball-on-flat tribometer equipped with a vacuum chamber and a current-controlling device, as shown in Fig. 1. The current-carrying friction tests were conducted at a speed of 5 cm/s, a reciprocating amplitude of 5 mm, a constant load of 5 N and DC electric currents of 0 A or 1 A. A steel ball (GCr15, with a diameter of 6 mm) was used as the counterpart. The friction tests started when the pressure of the chamber reached 5×10^{-3} Pa and stopped when the duration of the test reached 1800 s or the friction coefficient reached 0.3. The friction tests were repeated at least three times. The MOST films were further studied when the current was 1 A without sliding under the same experimental conditions.

2.3. General characterization of the films

The morphology of the original surfaces of the MOST films was analysed using a field emission scanning electron microscope (FESEM, Apreo S, Thermo Fisher Scientific, America), and the chemical compositions were evaluated using by a Kevex Sigma energy dispersive x-ray spectrometer (EDS). The films deposited on the Si substrates were destroyed to observe their cross-sectional morphology by the FESEM (SU8020, Hitachi, Japan). Four-point probe sheet resistance measurement (MCP-T610, Loresta-GP, Japan) was used to measure the electrical resistivity of the films deposited on the Si substrates; at least five areas were measured to reduce errors. The real-time contact voltage between the MOST films and the steel ball during friction was measured by a multimeter (Fluke 8846A, America). The hardness of the MOST films was measured with a nanoindenter (NHT^2, CSM, Switzerland) equipped with a Berkovich diamond probe tip. Each test was repeated at least five times to reduce errors.

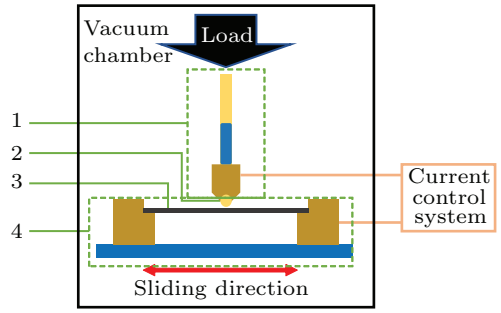


Fig. 1. Diagram of simple test device. 1. Fixture of counterface ball; 2. steel ball (6 mm); 3. sample; 4. fixture of the sample. The dark yellow color is copper, which has good conductivity, whilst the blue color represents the insulation.

2.4. General characterization of wear tracks and wear scars

The morphology of wear tracks on the films was analysed using FESEM (Apreo S, Thermo Fisher Scientific, America), and the chemical compositions were evaluated using the Kevex Sigma EDS. The surface of the counterface balls and films was investigated using an optical microscope (OM, Olympus STM6, Japan). Raman spectrometry (Raman, Renishaw, UK) equipped with a 532 nm laser was used to analyze the structure of the wear scars on the surfaces of the steel balls. The 3D morphology and cross-section profile of the wear tracks were observed, and the wear volume (V_m) was measured using a 3D non-contact surface profilometer (Micro XAM). The wear rate (W) can be calculated by

$$W = \frac{V_m}{F_n \cdot S}, \tag{1}$$

where V_m is the wear volume (mm^3), F_n is the normal load (N) and S is the sliding distance (m).

3. Results

3.1. Microstructure and properties of MOST films

The EDS was used to analyse the Ti content of the films. The results are shown in Table 1. The Ti content in the films increases with the increased sputtering current of the Ti target. The Ti content in the MOST films increases from 3.94 at.% to 15.98 at.% as the sputtering current of the Ti target increases from 0.2 A to 0.8 A. The electrical resistivity of pure MoS_2 is out of range, thereby showing that the MoS_2 film has very poor electrical conductivity. The electrical resistivity of the MOST films decreases with the increasing Ti content in the composite films. The results shows that Ti doping in MoS_2 is beneficial to improve the conductivity of MoS_2 films. Moreover, Ti doping in MoS_2 films improves their hardness, because of the solid solution hardening effect, reported by Teer *et al.*[11,12]

Table 1. Ti content, electrical resistivity, and hardness of films.

	MOST-0%Ti	MOST-4%Ti	MOST-8%Ti	MOST-12%Ti	MOST-16%Ti
Ti content in the film (at.%)	0	3.94	8.44	12.24	15.98
Electrical resistivity (Ω·m)	–	$(2.06\pm0.08)\times10^{-5}$	$(1.80\pm0.07)\times10^{-5}$	$(1.55\pm0.03)\times10^{-5}$	$(1.28\pm0.03)\times10^{-5}$
Hardness (GPa)	1.52±0.11	3.79±0.30	4.92±0.10	5.24±0.19	5.76±0.42

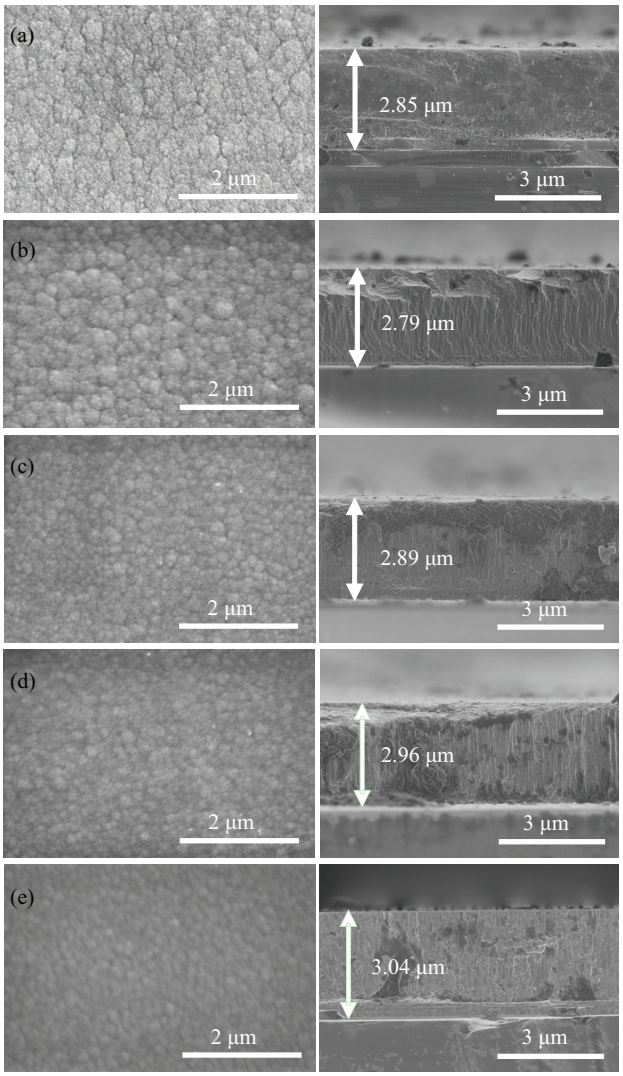


Fig. 2. FESEM images of surface and cross-sectional of films: (a) MOST-0%Ti; (b) MOST-4%Ti; (c) MOST-8%Ti; (d) MOST-12%Ti; (e) MOST-16%Ti.

Figure 2 shows the cross-sectional and surface morphology of the MOST films. In contrast to the MOST-0%Ti film, MoS_2 films show a decrease in the grain size with the increase of Ti doping. The films gain a dense columnar structure with the incorporation of Ti, and the special structure is beneficial to improve the mechanical properties of the films. Therefore, Ti doping can effectively improve the mechanical properties and reduce the grain size of MoS_2 films, as described in previous reports.[11,22–24] Interestingly, the thickness of the MOST-0%Ti film is similar to that of the MOST-8%Ti film despite having the shortest deposition time mainly because of the improved film compactness by Ti doping.

3.2. Vacuum tribological properties of MOST films under current-carrying

Figure 3(a) compares the friction coefficients of the MOST films when the current is 1 A. The pure MoS_2 film has a higher friction coefficient and a short wear life than the MOST composite films. The friction coefficient decreases and wear life increases when doping Ti in the film. However, the wear life is short when the Ti content increases to 16 at.%. This phenomenon indicates that an optimum Ti content improves the tribological properties of MoS_2 films when the current is 1 A. The real-time contact voltage between the films and the steel ball during friction was monitored with a computer, as shown in Fig. 3(b). The 3D morphology and cross-section profile of wear tracks are shown in Fig. 3(c). The contact voltages of MOST-0%Ti, MOST-4%Ti, and MOST-16%Ti had large fluctuations, but the contact voltages were kept at a relatively low level, which is originated from the failure of the films (Fig. 3(c)). Before the friction, 1 A current was applied in the contact area between the film and counterface, the contact voltage decreases with increasing the Ti content, which is consistent with the conductivity of films. Moreover, for the MOST-4%Ti, MOST-8%Ti, and MOST-12%Ti films, the contact voltages and friction coefficient are stable before 200 sliding cycles, indicating the films were not worn out in this stage. And the contact voltage decreases with increasing Ti content. Therefore, doping Ti can improve the electrical contact state of the film. In particular, the MOST-4%Ti film becomes worn out completely. However, it maintains a stable friction coefficient in the later stage of friction. The friction coefficient curve has an opposite trend with the contact voltage curves, that is, the friction coefficient increases as the contact voltage decreases. This interesting phenomenon is explained in the following discussion. The MOST-12%Ti film shows the local wear, which can cause the friction coefficient to fluctuate. The MOST-8%Ti has the lowest wear track depth, but its contact voltage is the highest.

To further analyse the differences in the tribological performances of the MOST films with different electrical conductivities under current-carrying conditions, the wear tracks of the films were observed by FESEM. The pure MoS_2 film shows flaky peeling on the edge of the wear track (Fig. 4(a)),

indicating strong adhesion is formed on the edge of wear track. The morphology of the wear track of MOST-4%Ti (Fig. 4(b)) is similar to that of MOST-0%Ti. With the increasing Ti content, the peeling on the edge of the wear track is not obvious. As shown in Fig. 4(c), the wear track only shows some ploughs, which indicates that the wear mechanism of the MOST-8%Ti film is mainly abrasive wear. The wear track of MOST-12%Ti has a discontinuous erosion pit inside the wear track. It implies that the wear mechanism of the MOST-12%Ti film is mainly adhesive wear. Figure 4(e) presents the EDS images of the wear track on MOST-12%Ti with a 1 A current. The depth of the partial area of the wear track on the MOST-12%Ti film is greater than the thickness of the film (Fig. 3(c)). The result can prove the occurrence of a local failure. Therefore, Fe in the failure area originates from the 304-stainless steel substrate. In addition, S and Ti are distributed in other areas evenly, and oxygen is minimal. The small amount of oxygen is due to the fact that oxidation does not easily occur in a vacuum environment.

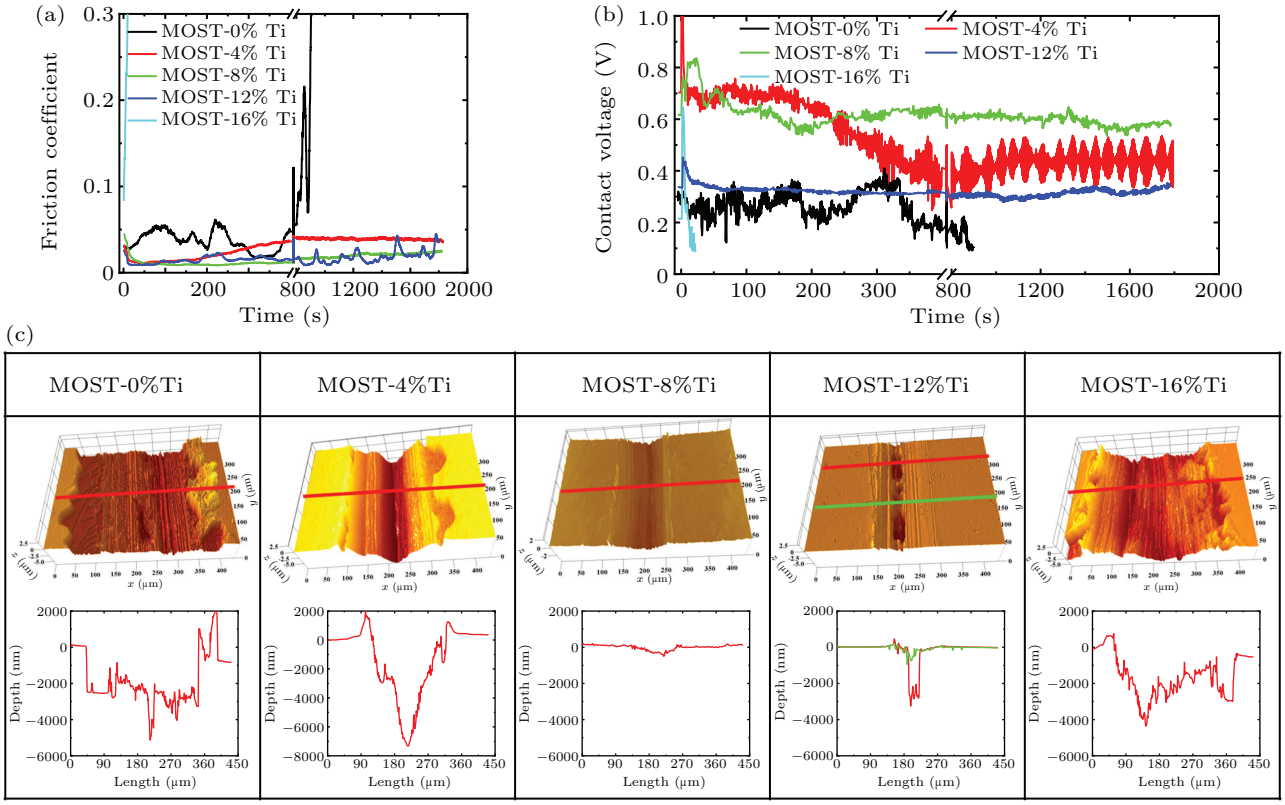


Fig. 3. (a) Friction coefficient curves, (b) contact voltage curves during friction, (c) 3D morphology and cross-section profile of wear tracks of MOST films under a current of 1 A.

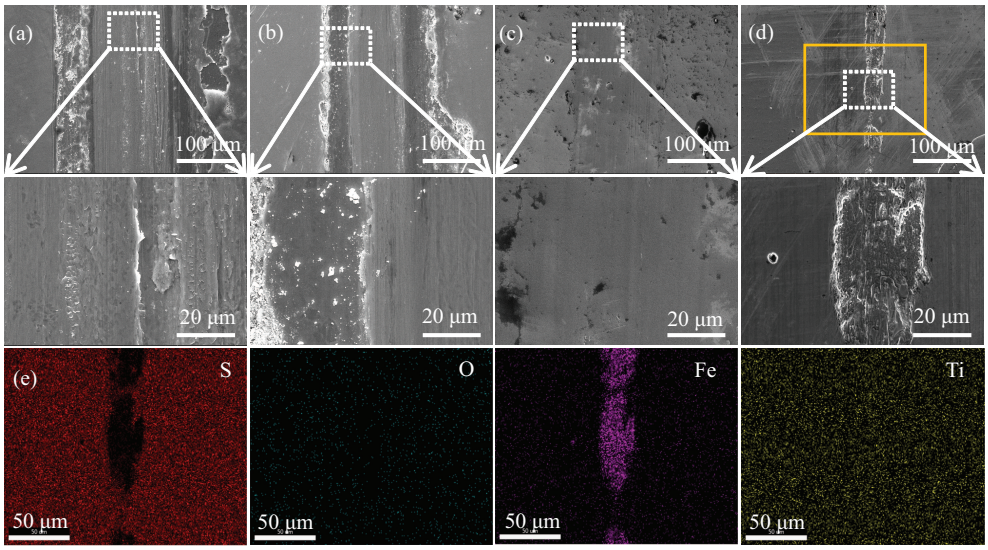


Fig. 4. FESEM image of wear tracks on films when the current is 1 A: (a) MOST-%Ti, (b) MOST-4%Ti, (c) MOST-8%Ti and (d) MOST-12%Ti; (e) energy dispersive spectroscopy images of yellow frame in (d).

3.3. Vacuum tribological properties of MOST films without current

The friction behavior of the MOST films without current was studied, as shown in Fig. 5. The pure MoS_2 has a higher friction coefficient than the Ti-doped MoS_2 films. Moreover, the wear rate decreases with increased Ti content when the current is 0 A. Therefore, Ti improves the wear resistance of the MOST films. However, the MOST-16%Ti film has the shortest wear life even under a current of 0 A. This result indicates that a large amount of titanium doping exerts a negative effect on the tribological properties of MoS_2 films.

Figure 6 shows the FESEM images of the wear tracks on the MOST films when the current is 0 A; these wear tracks only exist in some ploughs. With the increasing Ti content of the MOST films, the ploughs are not obvious because of the improved film hardness. The EDS images of the wear tracks on MOST-12%Ti without current are shown in Fig. 6(e). All elements are evenly distributed over the entire surface, including the surface and wear track. Thus, abrasive wear is mainly the wear mechanism when the current is 0 A.

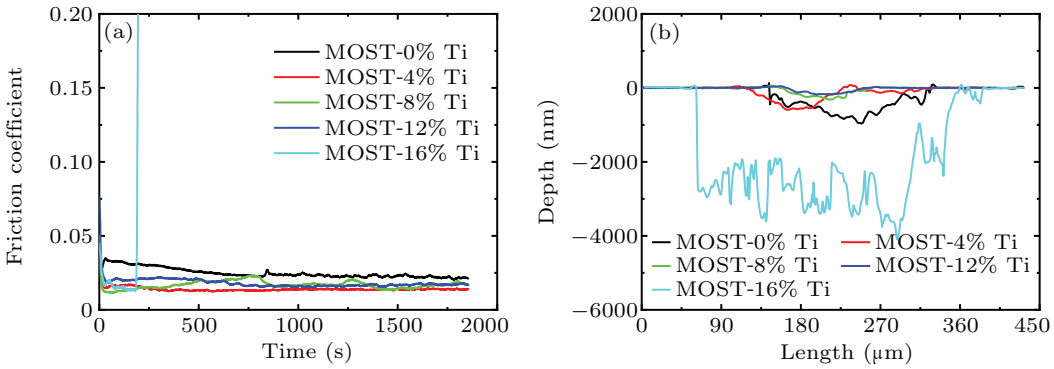


Fig. 5. (a) Friction coefficient curves and (b) cross-section profiles of wear tracks on MOST films under a current of 0 A.

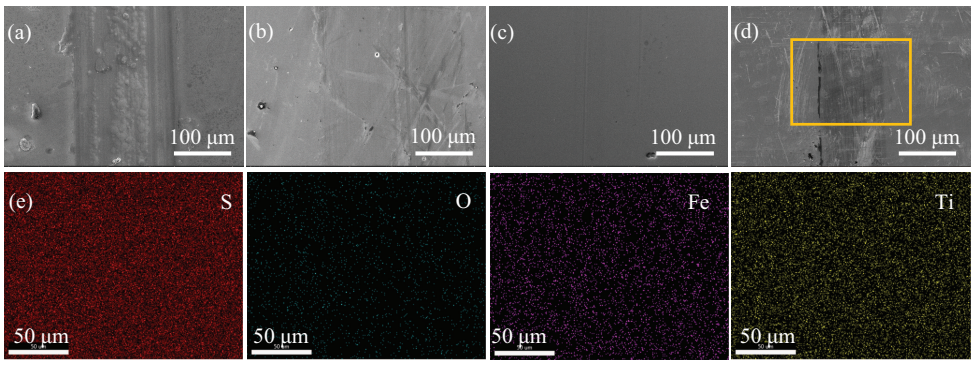


Fig. 6. FESEM image of wear tracks on films under a current of 0 A: (a) MOST-0%Ti, (b) MOST-4%Ti, (c) MOST-8%Ti and (d) MOST-12%Ti; (e) energy dispersive spectroscopy image of yellow frame in (d).

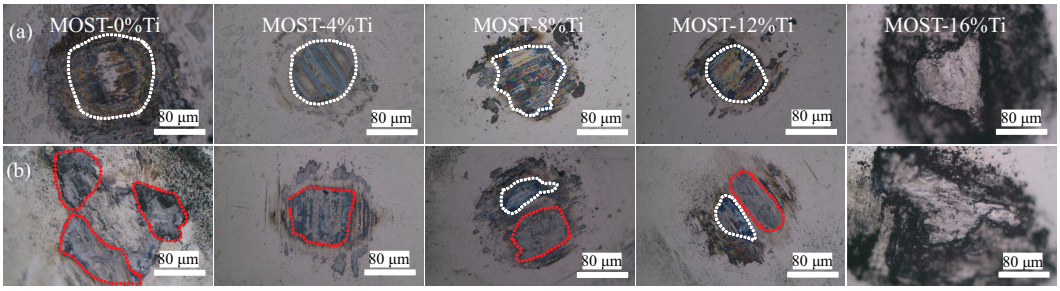


Fig. 7. Optical microscopic images of wear scars on the surface of the steel ball: (a) 0 A, (b) 1 A.

The morphology of the wear scars with and without current is clearly shown in Fig. 7. The morphology of the transfer films with a current seems to be thicker than that without a current. When the current is 1 A, the transfer film is gray (the area marked with a red circle) and inhomogenous (Fig. 7(b)). It is colored (marked by the white circle) and homogenous when the current is 0 A. The gray area indicates thicker transfer. Combined with the morphology of the wear tracks, the current caused the serious adhesive wear, thus promoting the local transfer from the film to the counterface and

forming a thick and inhomogenous transfer film in vacuum. Wang *et al.*[15,25] found that thick transfer films easily form under current-carrying conditions in air; hence, current could play the same role in different environments.

The average friction coefficient in the stable friction stage and wear rate under different conditions were compared, as shown in Table 2. The average friction coefficient and wear rate of the MOST films when the current is 0 A are lower than those in the condition with current, showing that th current has a negative effect on the tribological properties of the MOST films. The high wear rate under current-carrying originated from the strong adhesion wear. Moreover, the strong adhesion between film and counterface promotes the formation of thick and inhomogenous transfer film in vacuum, which is the main reason for the high and waved friction coefficient under current-carrying conditions. It is worth noting the wear difference of MOST-8%Ti and MOST-12%Ti films under different conditions; the wear rate of MOST-12%Ti film is lower than MOST-8%Ti film under non-current-carrying conditions, but the wear rate has an opposite trend under current-carrying even though the MOST-12%Ti film has better conductivity. Thus, the conductivity of the film is not the only factor that affects the current-carrying tribological properties of the film.

Table 2. The average friction coefficient and wear rate of MOST films.

		MOST-0%Ti	MOST-4%Ti	MOST-8%Ti	MOST-12%Ti	MOST-16%Ti
Average friction coefficient	0 A	0.025±0.003	0.014±0.001	0.017±0.002	0.018±0.002	0.016±0.006
	1 A	0.054±0.024	0.034±0.008	0.017±0.005	0.018±0.007	0.195±0.067
Wear rate ($mm^3/(N·m)$)	0 A	$(1.25±0.02)×10^{-6}$	$(0.53±0.06)×10^{-6}$	$(0.29±0.02)×10^{-6}$	$(0.18±0.01)×10^{-6}$	–
	1 A	–	–	$(0.61±0.02)×10^{-6}$	$(0.74±0.06)×10^{-6}$	–

3.4. Morphology of films and steel balls under the static current-carrying condition

A special experiment involving a static test was designed to understand the damage of current to film, as shown in Fig. 8. The morphology of the films and steel balls was observed using an optical microscope and a 3D non-contact surface profilometer (Fig. 9). The pure MoS_2 film is destroyed without sliding when the current is 1 A. This result is reflected in the depth of the cross-section profiles. The material transfer from the films to the steel ball. Moreover, molten droplets form on the surface of the MOST-0%Ti film and the corresponding steel ball, thereby showing that arc erosion occurs in this condition. With Ti doping in MoS_2 films, their resistivity is reduced, and they only show deformation under current-carrying. Therefore, the improvement of conductivity avoids the occurrence of current erosion. The degree of deformation of the films decreases with the increase of Ti content. According to Joule's first law, high resistance and current density generate more heat when the current passes through the contact area. The heat softens the film, which consequently deforms under a load of 5 N. The softened films are prone to adhesive wear. However, the MOST-12%Ti and MOST-16%Ti films have more obvious deformation than MOST-8%Ti, suggesting that the hardness of the film is a key factor in the current thermal effect. With increasing Ti content, the contact area becomes increasingly small because of the improvement of the film hardness. Current contraction occurs when the current passes the contact area of the steel ball and the film.[18,26] The lower contact area has an obvious current contraction, which results in high local current density. The high current density easily generates much heat, thereby softening the film and causing obvious deformation.

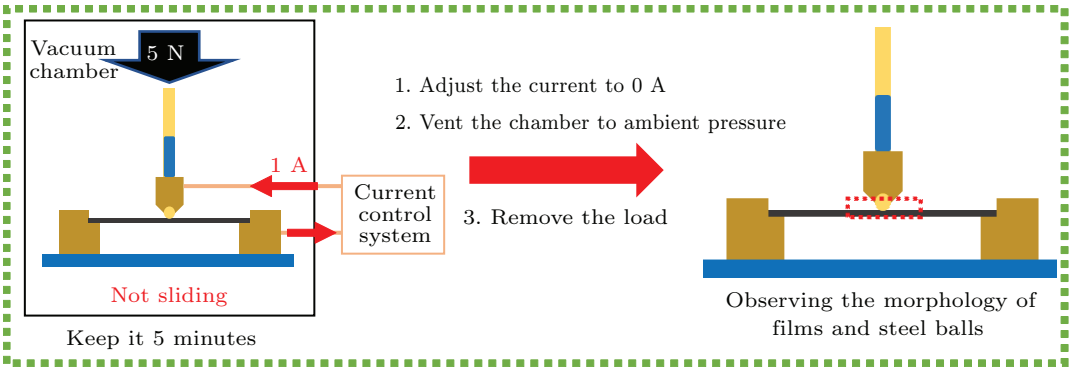


Fig. 8. Schematic of the static test.

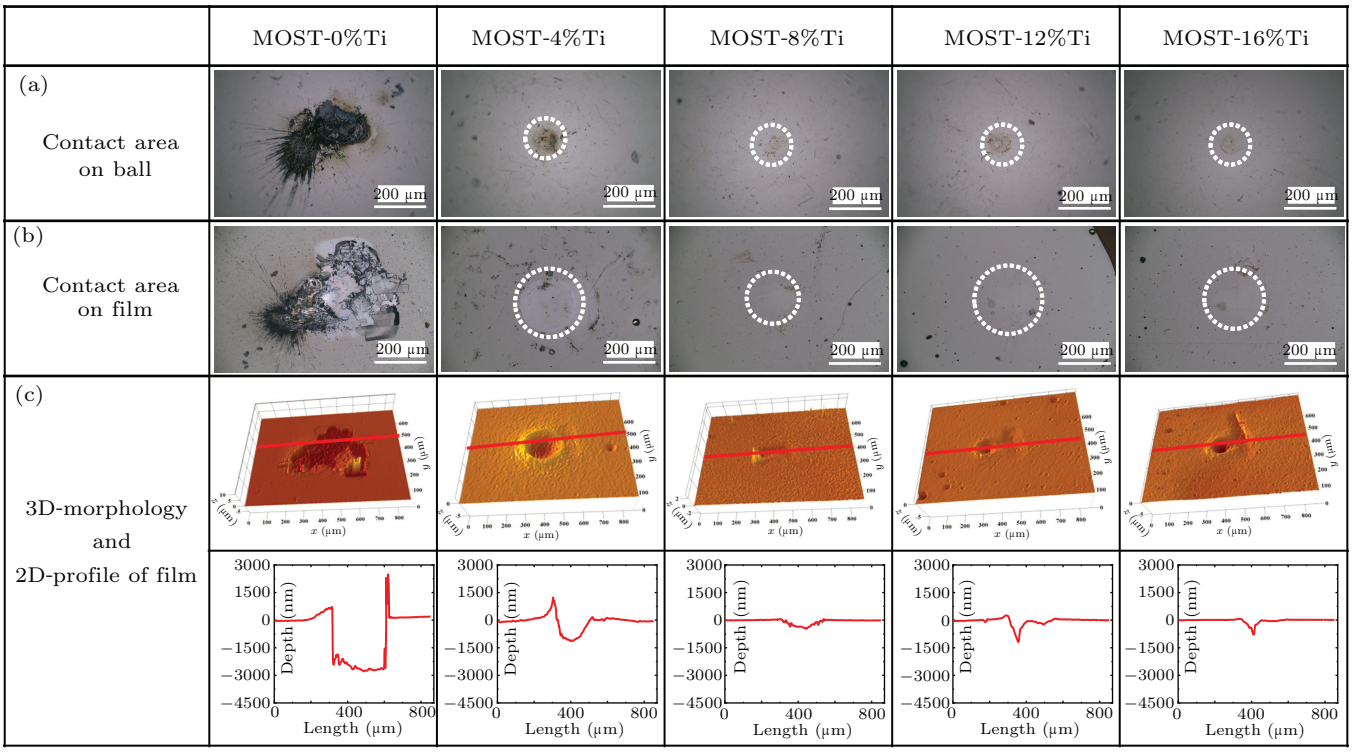


Fig. 9. The result of the static test. Optical microscopic images of contact area (a) on ball and (b) on film; (c) 3D morphology and 2D-profile images of films.

4. Discussion

The current-carrying tribological behavior of MOST composite films with different conductivities in vacuum was studied. As the complex wear mechanism when friction and current exist simultaneously, the current-carrying tribological mechanism of MOST films was analyzed from two views of mechanical wear and current erosion.

The results explicitly demonstrated that the MOST films with low Ti content had excellent tribological properties when the current was 0 A. In the static experiment, the change of voltage and current between the MOST-0%Ti film and the steel ball was monitored (Fig. 10). This process can be divided into three stages. In the first stage, the multimeter was turned on and recorded the numerical value. The contact voltage and contact current were zero because the voltage was not loaded. In the second stage, a voltage was applied to the friction pair, but the contact current was always zero due to the film's high resistance. As the constant current mode was set, the contact voltage would automatically increase until the film was instantly broken down. At this time, the direct contact between the steel substrate and the steel ball led to a sharp drop in contact resistance, and the third stage was entered: the current was constant at 1 A and the contact voltage was very low at about 100 mV. Therefore, the film was destroyed by the high voltage which caused the arc erosion,[27] explaining the molten splash at the contact area. Furthermore, the transfer film was formed on the surface of the steel ball even without sliding (Fig. 9(a)). Thus, before the beginning of friction, the current destroyed the film's structure and formed the contact between the transfer film and the steel substrate. Raman spectra were used to clarify the formation of the transfer film, as shown in Fig. 10(b). The transfer film included two main peaks at 374 cm^{-1} and 408 cm^{-1}, which indicated that the transfer film had a typical MoS_2 structure.[28,29] When the friction started, only the transfer film on the steel ball played a lubricating role, and thus maintained a high and waved friction coefficient for a certain period. The contact between the transfer film and the steel substrate led to a low contact voltage. When the transfer film in the contact area was completely worn off, the friction coefficient increased and the contact voltage decreased to the lowest value. The Raman peaks of MoS_2 were not obvious in the contact area of the steel ball when the friction coefficient increased to 0.3 (Fig. 10(c)). This result proved that the increase of the friction coefficient was due to the failure of the transfer film. The MOST-4%Ti film achieved a low friction coefficient and high contact voltage before 200 sliding cycles. However, the friction coefficient increased and the contact voltage decreased after 200 sliding cycles, which also had serious fluctuations. This is because the film has worn out, thus the friction coefficient increases due to lubrication failure. Moreover, the contact voltage was reduced due to the direct contact between the steel substrate and the steel ball, and poor lubricating contact after the wear-out of the film led to the fluctuation of the contact voltage. The transfer film remained when the friction stopped, so the friction coefficient did not increase further.

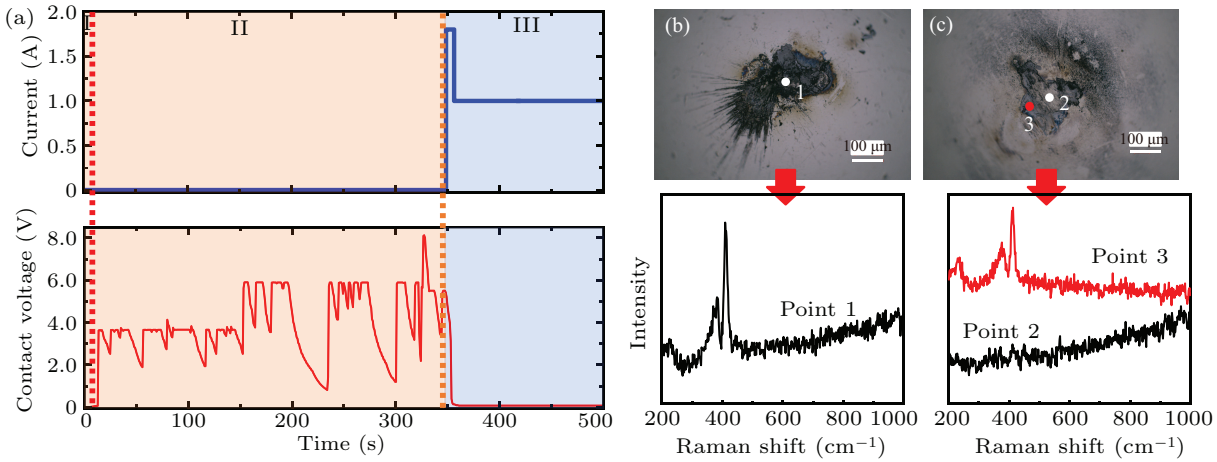


Fig. 10. (a) Curves of contact voltage and current between the MOST-0Ti% film and the steel ball in the static test; the morphology of the transfer film and the corresponding Raman spectrum under different conditions: (b) static tests; (c) friction with 1 A current.

The MOST-8%Ti film had excellent tribological properties under the currying-current condition, mainly ascribed to its good lubricity and conductivity. The current caused minimal damage to the MOST-8%Ti film (Fig. 9), which has the lowest wear rate. The current could not cause serious film deformation, so the friction coefficient was stable, and the main wear mechanism with the current was abrasive wear (Figs. 3(a) and 4(c)). As the film had better conductivity than MOST-4%Ti, the contact voltage was lower than that of MOST-4%Ti in the initial stage (Fig. 3(b)). Moreover, the film was not destroyed, and thus, the contact voltage was stable during friction.

The electrical resistance and contact voltage of the MOST-12%Ti film were lower than those of MOST-8%Ti. However, it had a more obvious deformation than MOST-8%Ti when the current existed without sliding. It originated from a small contact area caused by high hardness, leading to a local high current density. Then, more heat was generated, softening the film and promoting adhesion wear. Therefore, the stick-slip motion occurred, and a special morphology with local wear formed (Fig. 4(d)). Given a large amount of Ti-doped into MoS_2 films, the lubricity of the MOST-16%Ti film was insufficient. Moreover, it became easily worn out despite a current of 0 A. Thus, the MOST-16%Ti film had a short wear life regardless of the presence of a current.

The wear mechanism of MOST films in vacuum is not completely similar to that in an atmospheric environment. Wang *et al.* indicated that MOST films in an atmospheric environment with a current suffer from severe oxidation.[16] Yang *et al.* implied that the main wear mechanisms of copper matrix composites with a current are adhesion wear and arc erosion, as revealed in experiments conducted in extreme experimental conditions (e.g., too high electrical current density, too high sliding velocity).[21,30–32] However, in the vacuum condition in this study, oxygen was low such that the severe oxidation was not obvious. Moreover, the wear tracks did not show a large amount of oxygen, which indicated that oxidation wear was not the main mechanism of film failure in the vacuum environment. The pure MoS_2 film showed arc erosion due to poor conductivity, and the improvement of the electrical conductivity of the film inhibited the formation of an electric arc. Furthermore, flaky peeling on the edge of the wear track (Fig. 4(a)) and the discontinuous erosion pit inside the wear track (Fig. 4(d)) indicated the strong adhesion of the steel ball and films. Therefore, the wear mechanism of the MOST films with a current in vacuum was mainly adhesive wear, along with abrasive wear. Moreover, in this study, the serious adhesive wear depends on the current-induced arc erosion and the thermal effect. The arc erosion can avoid by improving the conductivity. While good conductivity and a large contact area are beneficial for minimizing the thermal effect.

5. Conclusion

This study deposited MoS_2-Ti composite films with different Ti contents by unbalanced magnetron sputtering system, studied the potential of MOST films as sliding electrical contact materials and revealed the vacuum tribological mechanism under current-carrying. The following conclusions are made.

(1) The conductivity and hardness of MOST films increase with increasing Ti content. Compared to traditional friction without current-carrying, the current-induced arc erosion and thermal effect take important roles in accelerating the wear. Doping Ti in the MoS_2 film can inhibit arc erosion due to the improved conductivity. While the thermal effect of current is mainly influenced by the conductivity and hardness of the film. The high hardness of the film causes a small contact area, thus forming a local high current density. Poor conductivity of the film and local high current density will generate more heat when the current passes through the film, which softens the film and causes adhesive wear. Thus, an optimum concentration of a Ti dopant results in minimal wear and preferential

lubricating behaviors due to the balance of conductivity and hardness.

(2) In particular, the MOST film with 8 at.% Ti exhibits excellent tribological properties when the current is 1 A, and its friction coefficient is 0.025, which is far lower than 0.2–0.3 for traditional precious metals. Thus, MoS_2-Ti films show great application potential as sliding electrical contact materials.

This study is beneficial for designing and developing sliding electrical contact materials.

Acknowledgements

Project supported by the National Natural Science Foundation of China (Grant No. 51775537) and Youth Innovation Promotion Association of Chinese Academy of Sciences (Grant No. Y202084).

References

[1] Braunovic M, Konchits V and Myshkin N 2007 *Electrical Contacts: Fundamentals, Applications and Technology* (CRC Press) p. 261
[2] Mogonye J E, Argibay N, Goeke R S, Kotula P G, Scharf T W and Prasad S V 2016 *Wear* **376–377** 1662
[3] Xie X L, Zhang L, Xiao J K, Qian Z Y, Zhang T and Zhou K C 2015 *Trans. Nonferrous Met. Soc. China.* **25** 3029
[4] Lee J, Kim H, Han K, Lee Y, Choi M and Kim C 2019 *ACS Appl. Mater. Interfaces* **11** 6276
[5] Serpini E, Rota A, Ballestrazzi A, Marchetto D, Gualtieri E and Valeri S 2017 *Surf. Coat. Tech.* **319** 345
[6] Stoyanov P, Chromik R R, Gupta S and Lince J R 2010 *Surf. Coat. Tech.* **205** 1449
[7] Colas G, Saulot A, Regis E and Berthier Y 2015 *Wear* **330–331** 448
[8] Fox V, Gampshire J and Teer D 1999 *Surf. Coat. Tech.* **112** 118
[9] Teer D G, Hampshire J, Fox V and Bellido-Gonzalez V 1997 *Surf. Coat. Tech.* **94–95** 572
[10] Gilmore R, Baker M A, Gibson P N and Gissler W 1998 *Surf. Coat. Tech.* **105** 45
[11] Renevier N M, Fox V C, Teer D G and Hampshire J 2000 *Surf. Coat. Tech.* **127** 24
[12] Rigato V, Maggioni G, Boscarino D, Sangaletti L, Depero L, Fox V C, Teer D and Santini C 1999 *Surf. Coat. Tech.* **116–119** 176
[13] Zhao H, Barber G C and Liu J 2001 *Wear* **249** 409
[14] Zhou K C, Xiao J K, Zhang L, Xie X L and Li Z Y 2015 *Wear* **326–327** 48
[15] Grandin M and Wiklund U 2013 *Wear* **302** 1481
[16] Wang P, Yue W, Lu Z B, Zhang G G and Zhu L N 2018 *Tribol. Int.* **127** 379
[17] Yang Z H, Zhang Y Z, Zhao F and Shanhguan B 2016 *Tribol. Int.* **94** 71
[18] Grandin M and Wiklund U 2018 *Wear* **398–399** 227
[19] Zhao H, Feng Y, Zhou Z J, Qian G, Zhang J C, Huang X C and Zhang X B 2020 *Wear* **444–445** 203156
[20] Generalova K N, Ryaposov I V and Shatsov A A 2016 *J. Frict. Wear* **37** 482
[21] Yang Z H, Ge Y X, Zhang X, Shangguan B, Zhang Y Z and Zhang J W 2019 *Materials* **12** 2881
[22] Qin X P, Ke P L, Wang A Y and Kim K H 2013 *Surf. Coat. Tech.* **228** 275
[23] Li H, Li X, Zhang G A, Wang L P and Wu G Z 2017 *Tribol. Lett.* **65** 38
[24] Lince J R, Hilton M R and Bommannavar A S 1995 *J. Mater. Res.* **10** 2091
[25] Wang Y F, Wang Y, Li X, Li A, Lu Z B, Zhang G A and Wu Z G 2019 *Tribol. Trans.* **62** 1119
[26] Yang H J, Chen G X, Gao G Q, Wu G N and Zhang W H 2015 *Wear* **332–333** 949
[27] Rieder W F 2000 *IEEE Trans Compon Packag Technol.* **23** 286
[28] Ky D L C, Tran Khac B C, Le C T, Kim Y S and Chung K H 2018 *Friction* **6** 395
[29] Windom B C, Sawyer W G and Hahn D W 2011 *Tribol. Lett.* **42** 301
[30] Xu W, Hu R, Li J S, Zhang Y Z and Fu H Z 2012 *Trans. Nonferrous Met. Soc. China* **22** 78
[31] Xiao Q D and Wu S 2014 *Adv. Appl. Ceram.* **113** 381
[32] Deng CY, Yin J, Zhang H B, Xiong X, Wang P, Sun M and Wu X G 2019 *Proc IMechE Part J: J Engineering Tribology* **233** 380